

# TPMCF: Temporal QoS Prediction using Multi-Source Collaborative Features

Suraj Kumar, Soumi Chattopadhyay, *Member, IEEE*, and Chandranath Adak, *Member, IEEE*

**Abstract**—In recent times, with the proliferation of online activities and the rapid deployment of web service APIs, personalized service recommendations have played a paramount role in the growth of the e-commerce industry. The performance of web services is one of the standard measures for service recommendation. Quality-of-Service (QoS) parameters determining the service performance fluctuate over time for a user. Thus, for a given user, the service QoS prediction over time plays an essential part in identifying a suitable service to invoke among a pool of services having the same functionality. The contemporary temporal QoS prediction methods hardly achieved the desired accuracy due to various limitations, such as data sparsity, the presence of outliers, and the inability to capture higher-order temporal relationships among user-service interactions. Even though some recent recurrent neural network-based sequential architectures can model temporal relationships among QoS data, the prediction accuracy degrades due to the absence of other features (e.g., collaborative self features, collaborative spatial features of users/services) to comprehend the relationship among the user-service interactions. In addition to the lack of effective representation of implicit features, having the same attention across all the features in every timestep may impede improving the prediction accuracy. This paper addresses the above challenges and proposes a scalable strategy for Temporal QoS Prediction using Multi-source Collaborative Features (namely, TPMCF) enabling faster responsiveness while attaining high prediction accuracy. Our work combines the collaborative features of the user/service by exploiting the user-service relationship with the spatio-temporal auto-extracted features by employing graph convolution and a variant of transformer encoder with multi-head self-attention. While the graph convolutional is responsible for automatic feature extraction exploiting the spatial information, the transformer encoder is accountable for capturing the temporal dependency among QoS data for prediction. We validated our proposed method on WS-DREAM-2 benchmark datasets. Extensive experiments showed that TPMCF outperformed the major state-of-the-art approaches in terms of prediction accuracy while ensuring high scalability and reasonably faster responsiveness.

**Index Terms**—Temporal QoS Prediction, Multi-Head Attention, Graph Convolutional Matrix Factorization, Transformer Encoder

## 1 INTRODUCTION

Over the years, the Internet has been floating with important as well as nominal information on the world wide web (www). Understanding the users' experiences and providing personalized recommendations, most business applications have started adopting service-oriented architectures [1]. According to a leading web-service API monitoring forum (programmableweb.com), more than 24,500 services APIs meandering from e-commerce to transportation to gaming have been deployed over the Internet. With the rapid deployment of services, selecting an appropriate service from a vast API repository comprising functionally indistinguishable services for a user is becoming time/resource-consuming, leading to high costs if chosen one by one. Therefore, service recommendation to an intended user, while fulfilling the user-satisfaction level, is one of the fundamental research problems in services computing [2].

One of the standard practices is to recommend service based on values of Quality-of-Service (QoS) parameters since QoS parameters (e.g., response time, throughput) are generally used to assess the performance of web services.

However, the QoS parameters are not fixed entities for a service. They vary across users, as shown in Figure 1(a). Even for a specific user, the QoS fluctuates over time, as depicted in Figure 1(b). Therefore, QoS prediction becomes necessary before recommending a service, which is the primary focus of this paper.

Many contemporary methods focus on solving QoS prediction across users while ignoring the temporal dependencies among QoS values [4], [5]. The long-established approaches used for the static QoS prediction are based on collaborative filtering (CF) [6], which are classified into three categories: (a) memory-based approaches using similarity between users and services [7], [8], [9], (b) model-based approaches using matrix factorization (MF) [10], [11]/ factorization machine [12], [13]/ deep-architectures [5], and (c) hybrid methods combining both memory and model-based approaches [4], [14]. Altogether these approaches explicitly use features such as the similarity between users/services, statistical parameters obtained from the QoS invocation logs of users/services, and contextual information (e.g., geographical locations, network locations/ attributes) to exploit the low-level to high-level features. However, these approaches are modeled to predict the QoS value while neglecting the temporal context of QoS data. The static QoS prediction methods are apparently insufficient for making accurate QoS predictions because most of the QoS parameters fluctuate over time, even for a specific user-service pair, as presented in Figure 1(b).

- S. Kumar and S. Chattopadhyay are with the Department of CSE, Indian Institute of Information Technology Guwahati, India-781015. e-mail: {suraj.kumar, soumi}@iiitg.ac.in.  
C. Adak is with the Indian Institute of Technology, Patna, India-801106. e-mail: chandranath@iiitp.ac.in  
This work has been submitted to the IEEE for possible publication. Copyright may be transferred without notice, after which this version may no longer be accessible.

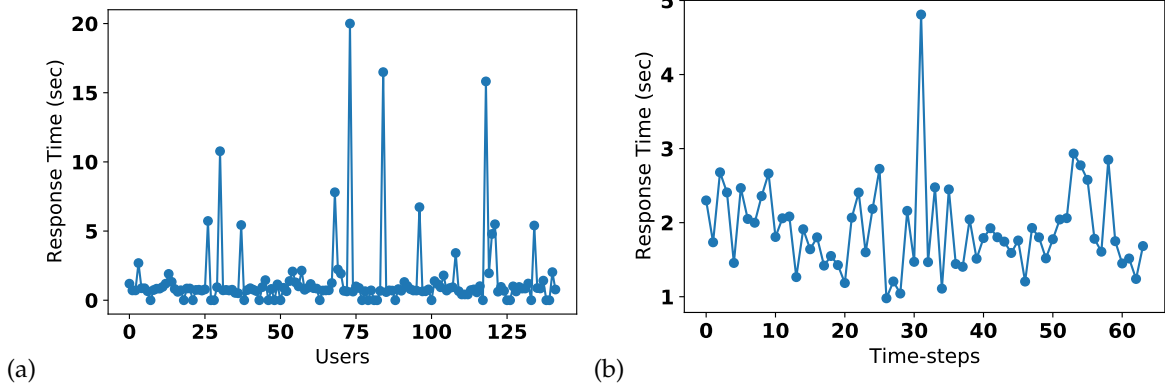


Fig. 1: QoS variation of service across (a) users and (b) time-steps. Data from WSDREAM-2 dataset [3]

Recently, a few methods have addressed the temporal aspect of QoS prediction by modeling it using various means. One of the popular techniques for temporal QoS prediction is based on temporal smoothing (TS) [15], [16], [17]. In general, TS-based techniques employ the data imputation using static CF-based methods to fill up the missing values at a specific time-step followed by computing the weighted average across the previous few time-steps for predicting the QoS at the given time-step. However, the TS-based methods do not usually exploit the temporal features accurately, leading to prediction accuracy degradation. Therefore, the ARIMA-based model [18] employing time-series forecasting has been proposed. However, the ARIMA-based methods are computationally expensive and less explainable than TS. Further, similar to MF, tensor factorization (TF)-based models [19], [20], [21], [22], [23] have been proposed to exploit the triadic relationship among user, service, and time. However, these models are unable to capture the high-dimensional complex features among the QoS invocation sequences. A few recent studies using deep learning (e.g., Long Short Term Memory (LSTM) [24], [25], [26], [27], [28], Gated Recurrent Unit (GRU) [29], [30])-based models have claimed to achieve improvement in prediction accuracy over traditional approaches. However, the inability to capture the complex and higher-order triadic relationship among user-service interactions over time due to inadequate feature representation causes performance degradation for these deep learning-based methods. Most of the deep learning-based methods in the literature use either *QoS features* derived from the temporal QoS invocation log matrix [15], [16], or the *contextual features* (e.g., geographical location, network parameters, like IP address, autonomous system) for the target user/service to predict the QoS value [27], [28]. However, to improve the prediction accuracy, the user/service interactions are required to be explored thoroughly.

Considering the above limitations observed in the literature, this paper proposes a framework (TPMCF), which leverages the Graph Convolution [31] followed by Transformer Encoder [32] to exploit the spatio-temporal collaborative features capturing the triadic relationship across the temporal QoS invocation sequences. To the best of our knowledge, TPMCF is the earliest attempt in the domain of QoS prediction that (a) captures the multi-source collaborative features for the temporal QoS prediction to

improve the prediction accuracy, (b) leverages a transformer encoder with multi-head attention to capture the temporal dependency among QoS data. As evident from our experimental studies, TPMCF outperformed major state-of-the-art methods in terms of prediction accuracy. Moreover, TPMCF attained better prediction accuracy with multi-source collaborative features than the methods using handcrafted or auto-extracted spatial/temporal features independently. Furthermore, our temporal QoS prediction module containing a transformer encoder performed better than the other sequential networks, such as LSTM or GRU that have been widely used for temporal prediction due to its self-attention mechanism. We now summarize our **contributions** below.

(i) *Utilization of multi-source collaborative features for QoS prediction*: TPMCF thoroughly exploits collaborative features of users and services to capture complex, higher-order relationships among user-service interactions over time to attain high prediction accuracy. On the one hand, TPMCF combines explicit features derived using domain knowledge with auto-extracted features for the target user-service pair. On the other hand, TPMCF auto-extracts spatial features by exploring neighborhood relationships along with the temporal features by analyzing the user-service interactions over time.

(ii) *Spatial feature extraction using graph convolution*: We propose a graph convolutional matrix factorization (GCMF) module to auto extract spatial features by exploring the neighborhood of the given user-service pair. On the one hand, GCMF addresses the issue of data sparsity, which is one of the most prominent problems in the domain of temporal QoS prediction [2]. On the other hand, GCMF is able to capture complex relationships among QoS data, leading to more accurate QoS prediction.

(iii) *QoS prediction using a transformer encoder*: We further propose a temporal QoS prediction module comprising a transformer encoder followed by a fully connected neural network. In general, the transformer encoder works better than LSTM [26] and GRU [29]-based sequential architectures due to its self-attention mechanism [32], as observed empirically. In this paper, we adopt the transformer encoder architecture [32] and propose an improvised version, namely, the predictive transformer encoder (PTE), responsible for capturing the temporal dependencies among QoS data. The PTE takes a sequence of the spatial features for a given user-

service pair, extracted by the GCMFs and generates spatio-temporal features by exploiting the temporal dependencies among the feature sequences, which is the earliest attempt of its kind. A fully connected neural network finally uses the spatio-temporal features for prediction.

(iv) *Extensive experiments*: We performed an extensive experiment on two benchmark datasets of WSDREAM-2 [3]. Experimental results show that our framework outperformed major state-of-the-art approaches in terms of prediction accuracy.

The rest of the paper is organized as follows. Section 2 presents an overview of the problem formulation. Section 3 then discusses the proposed framework in detail. The experimental results are analyzed in Section 4, while the literature review is presented in Section 5. Finally, Section 6 concludes this paper.

## 2 PROBLEM FORMULATION

Figure 2 represents the pictorial overview of the temporal QoS prediction problem, which is mathematically formulated in this section. Given the following inputs to the framework:

- A set of  $n$  users  $\mathcal{U} = \{u_1, u_2, \dots, u_n\}$
- A set of  $m$  services  $\mathcal{S} = \{s_1, s_2, \dots, s_m\}$
- A QoS parameter  $q$
- A set of observations on  $q$  for user-service pair  $(u_i, s_j) \in \mathcal{U} \times \mathcal{S}$  for past  $T$  time-steps
- A QoS invocation log  $\mathcal{Q}$  in the form of a tensor with dimension  $n \times m \times T$ , as defined below:

$$\mathcal{Q}(i, j, t) = \begin{cases} q_{ij}^t \in \mathbb{R}_+ & \text{value of } q \text{ of } s_j \text{ invoked by } u_i \\ & \text{at } t^{\text{th}} \text{ time-step} \\ 0 & \text{Otherwise (representing inv-} \\ & \text{alid entry)} \end{cases}$$

The objective is to predict the value of  $q$  for a target user-service pair  $(u_i, s_j)$  at the time-step  $T$ .

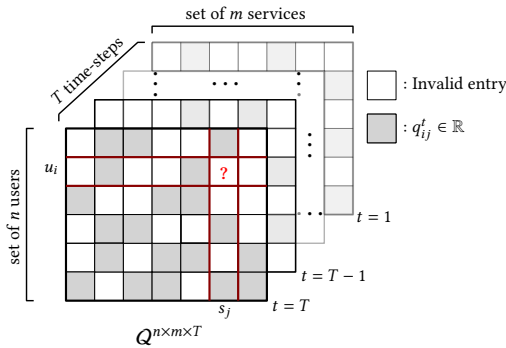


Fig. 2: Temporal QoS prediction

## 3 TPMCF: PROPOSED FRAMEWORK

This section discusses our proposed framework TPMCF for temporal QoS prediction. TPMCF has two primary modules: (a) *Collaborative spacial feature extraction module (CSFE)*: responsible for extracting spatial features using graph convolutional matrix factorization (GCMF), and (b) *Temporal QoS prediction module (TQP)*: accountable for generating spatio-temporal features utilizing a variant of transformer encoder,

followed by QoS prediction using a fully connected neural network. Given initial feature vectors of a user-service pair  $u_i, s_j$  at a specific time-step, GCMF exploits the neighborhood of  $u_i$  and  $s_j$ , and extracts spatial features that PTE then employs to generate spatio-temporal features to be used by a fully connected neural network for QoS prediction. Other than spatial feature extraction to enable the framework to achieve a high prediction accuracy, GCMF has another significant advantage when employed prior to the transformer encoder. GCMF handles the data-sparsity issues quite well. Therefore, we do not require any additional data imputation method to predict the missing values, which could impede achieving high prediction accuracy when any deep neural architecture does the estimation. We now explain each module of TPMCF in detail. We begin by describing the QoS invocation graph representation, which is one of the primary components the CSFE module of TPMCF.

### 3.1 Representation of QoS Invocation Graph

We first define the QoS invocation graph (QIG).

**Definition 3.1** (QoS Invocation Graph (QIG)). A QoS invocation graph  $\mathcal{G}^t = (U^t \cup S^t, E^t, \mathcal{U}\mathcal{E}^t \cup \mathcal{S}\mathcal{E}^t)$  is a bipartite graph, where the vertices  $U^t$  and  $S^t$  represent the set of users  $\mathcal{U}$  and the set of services  $\mathcal{S}$ , respectively. An edge  $e_{ij}^t = (u_i^t, s_j^t) \in E^t$  exists between two vertices,  $u_i^t \in U^t$  and  $s_j^t \in S^t$ , if  $\mathcal{Q}(i, j, t) = q_{ij}^t \neq 0$ . Each node  $u_i^t \in U^t$  and  $s_j^t \in S^t$  are associated with node vectors  $\mathcal{U}\mathcal{E}_i^t \in \mathcal{U}\mathcal{E}^t$  and  $\mathcal{S}\mathcal{E}_j^t \in \mathcal{S}\mathcal{E}^t$  representing the initial feature embedding of  $u_i$  and  $s_j$  at time-step  $t$ , respectively. ■

An example of a QIG at time-step  $t$  is shown in Figure 3(a). In CSFE module, a QIG  $\mathcal{G}^t$  is represented by an adjacency matrix  $\mathcal{A}^t$  of dimension  $N \times N$ , where  $N = n + m$ , as defined below.

$$\mathcal{A}^t = (a_{ij}^t) \in \{0, 1\}^{N \times N}; \quad a_{ij}^t = \begin{cases} 1, & \text{if } e_{ij}^t \in E^t \text{ of QIG } \mathcal{G}^t \\ 0, & \text{otherwise} \end{cases}$$

The adjacency matrix  $\mathcal{A}^t$  helps to explore the neighborhood of each node to generate the spatial feature embedding for all the users and services. However, instead of using  $\mathcal{A}^t$  directly in the CSFE module, we normalize  $\mathcal{A}^t$  (denoted by  $\bar{\mathcal{A}}^t$ ) as follows.

$$\bar{\mathcal{A}}^t = (\mathcal{D}^t)^{-\frac{1}{2}} (\mathcal{A}^t + \mathbb{I}_{N \times N}) (\mathcal{D}^t)^{-\frac{1}{2}} \quad (1)$$

Where  $\mathcal{D}^t$  is a diagonal matrix representing the degree of each node of  $\mathcal{G}^t$  by its diagonal elements, as defined below.

$$\mathcal{D}^t = (d_{ij}^t) \in \mathbb{Z}_+^{N \times N}; \quad d_{ij}^t = \begin{cases} 1 + \sum_{k=1}^N \mathcal{A}^t(i, k), & \text{if } i = j \\ 0, & \text{otherwise} \end{cases}$$

Normalization is required here to avoid the more significant influence of the higher-degree nodes during learning [31]. This is because the higher degree nodes do not necessarily mean they contribute more to the prediction. It only means they have more interactions at that time-step. Moreover, normalization helps in scaling. In Eq. 1, an identity matrix (i.e.,  $\mathbb{I}_{N \times N}$ ) is added to take into account the self-influence of a node while extracting the spatial features for it. It may be noted, each non-zero element of  $\bar{\mathcal{A}}^t$ , i.e.,  $\bar{\mathcal{A}}^t(i, j)$ , is normalized by the square root of the number of invocations

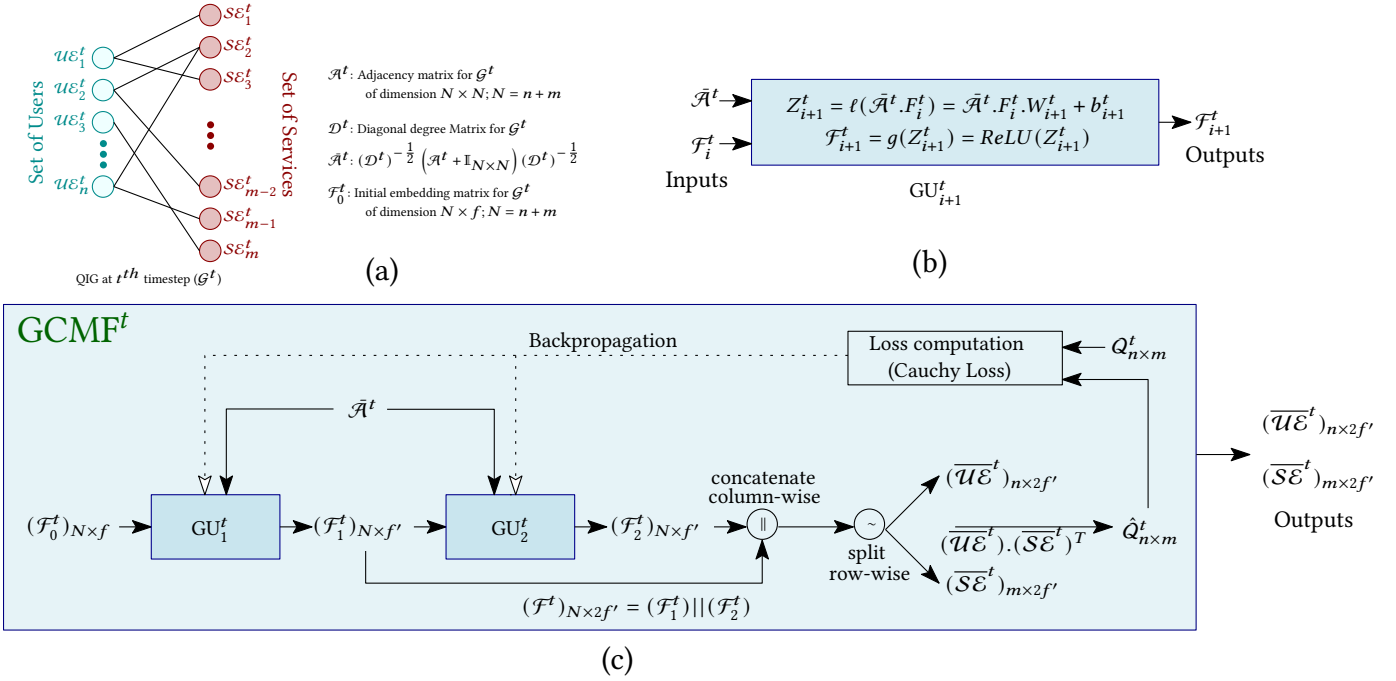


Fig. 3: Collaborative spatial feature extraction module using graph convolutional matrix factorization (GCMF)

of the corresponding user  $u_i$  and service  $s_j$  at time-step  $t$  as recorded in  $\mathcal{Q}$ , refers to Eq. 2.

$$\bar{\mathcal{A}}^t(i, j) = \frac{\mathcal{A}^t(i, j)}{\sqrt{d_{ii}^t} \cdot \sqrt{d_{jj}^t}} \quad (2)$$

$\bar{\mathcal{A}}^t$  is finally used for the convolution operation in the CSFE module, which is discussed later in this section.

As mentioned in Definition 3.1, each node in  $(U^t \cup S^t)$  is associated with a node vector representing the feature embedding of the corresponding user or service. We now discuss the construction of the initial feature embedding for the users/services below.

### 3.1.1 Construction of Initial Feature Embedding

The initial feature embedding of a user or service consists of three different types of feature vectors obtained from  $\mathcal{Q}$ , as discussed below.

(i) *Statistical Features ( $\mathcal{F}_S^t$ )*: For each user  $u_i \in \mathcal{U}$  or service  $s_j \in \mathcal{S}$ , we obtain the statistical features  $\mathcal{F}_S^t(u_i)$  or  $\mathcal{F}_S^t(s_j)$  consisting of five statistical parameters: minimum, maximum, median, mean, and standard deviation from their QoS invocation profile  $\mathcal{Q}^t(u_i)$  or  $\mathcal{Q}^t(s_j)$ , where  $\mathcal{Q}^t(u_i) = \mathcal{Q}(i, \cdot, t)$  and  $\mathcal{Q}^t(s_j) = \mathcal{Q}(\cdot, j, t)$  represent the QoS invocation vectors of  $u_i$  and  $s_j$  at time-step  $t$ , respectively. Statistical features of a user or service capture the global characteristics of the invocation pattern of that user or service.

(ii) *QoS Features ( $\mathcal{F}_Q^t$ )*: We use matrix decomposition [10] of  $\mathcal{Q}^t$  (i.e., QoS invocation log matrix at  $t$ ) to obtain the QoS feature embedding of length  $f_q$  for each user and service (say,  $\mathcal{F}_Q^t(u_i)$  and  $\mathcal{F}_Q^t(s_j)$ ) at  $t$ .

(iii) *Collaborative features using correlations ( $\mathcal{F}_C^t$ )*: For each user  $u_i \in \mathcal{U}$  or service  $s_i \in \mathcal{S}$ , we first obtain the correlation between  $u_i$  or  $s_i$  and every other user  $u_j \in \mathcal{U}$  or service

$s_j \in \mathcal{S}$  in terms of their QoS invocation profile  $\mathcal{Q}^t(u_i)$  or  $\mathcal{Q}^t(s_j)$  using cosine similarity [33]. It may be noted that for each  $u_i$  or  $s_i$ , we have a vector of length  $n$  or  $m$ , which is then fed to a stacked autoencoder [34] to obtain the latent representation of correlation feature embedding of length  $f_c$  for each user and service (say,  $\mathcal{F}_C^t(u_i)$  or  $\mathcal{F}_C^t(s_j)$ ) at  $t$ .

The final feature embedding for a user  $u_i$  or service  $s_j$  is constructed by concatenating the above three feature vectors.

$$\mathcal{U}\mathcal{E}_i^t = \mathcal{F}_S^t(u_i) \parallel \mathcal{F}_Q^t(u_i) \parallel \mathcal{F}_C^t(u_i)$$

$$\mathcal{S}\mathcal{E}_j^t = \mathcal{F}_S^t(s_j) \parallel \mathcal{F}_Q^t(s_j) \parallel \mathcal{F}_C^t(s_j)$$

The initial feature embedding matrix  $\mathcal{F}_0^t$  is of dimension  $N \times f$ , where  $f = 5 + f_q + f_c$ . The first  $n$  rows of  $\mathcal{F}_0^t$  contain user-feature embedding for  $n$  users, while the last  $m$  rows of  $\mathcal{F}_0^t$  comprise service-feature embedding for  $m$  services. This embedding matrix  $\mathcal{F}_0^t$  is used in the CSFE module to incorporate neighborhood information for every user/service.

## 3.2 Collaborative Spatial Feature Extraction (CSFE) Module using GCMF

We now discuss the automated feature generation using GCMF at time-step  $t$ . Figure 3(b) shows the details of a GCMF-unit (GU), which is the core component of the CSFE module. Given the normalized adjacency matrix  $\bar{\mathcal{A}}^t$  and feature embedding matrix  $\mathcal{F}_i^t$  to the  $i^{\text{th}}$  GCMF-unit ( $\text{GU}_i^t$ ), for each node  $v_j^t \in U^t \cup S^t$  of  $\mathcal{G}^t$ ,  $\text{GU}_i^t$  combines the feature of  $v_j^t$  with the features of all the nodes reachable from  $v_j$  with a path length less than or equal to  $i$  to obtain spatial feature vector for  $v_j^t$ .

In our CSFE module, two GUs are connected sequentially. The output of  $\text{GU}_1^t$  (i.e.,  $\mathcal{F}_1^t$ ) is concatenated with the output of  $\text{GU}_2^t$  (i.e.,  $\mathcal{F}_2^t$ ) to obtain a matrix  $\mathcal{F}^t$  of size  $N \times 2f'$ .

Finally,  $\mathcal{F}^t$  is split row-wise to generate user and service embedding matrices,  $\overline{U}\mathcal{E}^t$  and  $\overline{S}\mathcal{E}^t$ , respectively. Figure 3(c) presents the overview of the GCMF architecture. The output of the CSFE module is forwarded to the subsequent module of our framework.

### 3.3 Temporal QoS Prediction (TQP) Module using Predictive Transformer Encoder (PTE)

This is the final module of our framework. Given a target user-service pair  $u_i$  and  $s_j$ , the objective of this module is to predict the QoS value for  $u_i, s_j$  at time-step  $t$ . The main crux of this module is to predict the value of  $\mathcal{Q}(i, j, k)$  while considering the temporal dependencies for the last  $\mathcal{T}$  time-steps.

The first step of this module is to generate the input embedding, which is then fed to a series of transformer encoder blocks, followed by global max-pooling and fully connected (FC) layers to predict the value of  $\mathcal{Q}(i, j, k)$ . The pictorial overview of this module is shown in Figure 4(a). We now discuss each step in detail.

#### 3.3.1 Input Embedding Construction

At first, for each time-step  $k$  (where,  $t - \mathcal{T} + 1 \leq k \leq t$ ), the user embedding  $\overline{U}\mathcal{E}_i^k \in \overline{U}\mathcal{E}^k$  and the service embedding  $\overline{S}\mathcal{E}_j^k \in \overline{S}\mathcal{E}^k$  obtained from the CSFE module are concatenated to produce a vector  $\overline{\mathcal{E}}_{ij}^k$  of length  $4f'$ . Finally,  $\overline{\mathcal{E}}_{ij}^k$  across all  $\mathcal{T}$  time-steps are concatenated row-wise to generate the input embedding  $\mathcal{I}\mathcal{E}_{ij}^t$  of dimension  $\mathcal{T} \times 4f'$ .

$$\mathcal{I}\mathcal{E}_{ij}^t = \underbrace{(\overline{U}\mathcal{E}_i^{t-\mathcal{T}+1} \parallel \overline{S}\mathcal{E}_j^{t-\mathcal{T}+1})}_{\overline{\mathcal{E}}_{ij}^{t-\mathcal{T}+1}} \parallel \dots \parallel \underbrace{(\overline{U}\mathcal{E}_i^{t-1} \parallel \overline{S}\mathcal{E}_j^{t-1})}_{\overline{\mathcal{E}}_{ij}^{t-1}} \parallel \underbrace{(\overline{U}\mathcal{E}_i^t \parallel \overline{S}\mathcal{E}_j^t)}_{\overline{\mathcal{E}}_{ij}^t}$$

#### 3.3.2 Training of PTE

We train the PTE with the input embedding  $\mathcal{I}\mathcal{E}_{ij}^t$  and target value  $q_{ij}^t$ , for all  $u_i, s_j$  such that  $\mathcal{Q}(i, j, t) \neq 0$ . Figure 4(b) presents the detail of our transformer encoder network. The core component of PTE is multi-head attention (MHA) with  $h$  heads as presented in Figure 4(c). Each head of MHA comprises scaled dot-product attention (SDPA) [32], which is presented in Figure 4(d). The objective of the MHA block is to compute the attention required to give each part of the input across different time-steps. Each head  $i$  (where  $i \in \{1, 2, \dots, h\}$ ) of MHA computes a tuple comprising query, key, and value, i.e.,  $(Q^i, K^i, V^i)$  as shown below.

$$\begin{aligned} (Q^i)_{\mathcal{T} \times d_k} &= (\mathcal{I}\mathcal{E}_{ij}^t)_{\mathcal{T} \times 4f'} (W_Q^i)_{4f' \times d_k} \\ (K^i)_{\mathcal{T} \times d_k} &= (\mathcal{I}\mathcal{E}_{ij}^t)_{\mathcal{T} \times 4f'} (W_K^i)_{4f' \times d_k} \\ (V^i)_{\mathcal{T} \times d_v} &= (\mathcal{I}\mathcal{E}_{ij}^t)_{\mathcal{T} \times 4f'} (W_V^i)_{4f' \times d_v} \end{aligned} \quad (3)$$

The tuple  $(Q^i, K^i, V^i)$  is then forwarded to the SDPA block, which is responsible for computing the attention for the input sequence across  $\mathcal{T}$  time-steps. The outcomes of each SDPA block of size  $\mathcal{T} \times d_v$  are now concatenated column-wise across all heads, and fed to the next block to perform a linear operation with weight matrix  $W_L$ . It may be noted, the MHA block produces an output of size  $\mathcal{T} \times 4f'$ .

The PTE comprises a residual connection that adds the output generated by MHA with  $\mathcal{I}\mathcal{E}_{ij}^t$ , which is then passed

through a layer normalization (LN) [32], [35]. The output of this LN is then fed to two 1D convolution layers (Conv1D) connected sequentially. In between these two Conv1D layers, we use a dropout layer for regularization [35]. The output of the second Conv1D is added to the output of the previous LN, which is then fed to another LN to generate the final output vector of the PTE.

In the temporal QoS prediction module, the input embedding passes through  $C_1$  number of PTE blocks sequentially. The output vector of the final PTE block is fed to a global max pooling layer, which is then forwarded to  $C_2$  number of fully connected layers to predict the value  $\hat{q}_{ij}^t$ . A detailed configuration of the temporal QoS prediction module is presented in Section 4.

### 3.4 Outlier Detection and Handling

The QoS prediction accuracy is highly sensitive to the outliers present in the dataset [20]. In this paper, we employ two different strategies to handle the outliers. To train GCMF and PTE, we use Cauchy loss [36] to handle outliers, as presented in Eq.s 4 and 5, respectively.

$$\mathcal{L}_{GCMF}^k = \sum_{q_{ij}^k \neq 0} \log \left( 1 + \frac{(q_{ij}^k - \hat{q}_{ij}^k)^2}{\gamma_s^2} \right) \quad (4)$$

$$\mathcal{L}_{PTE} = \sum_{q_{ij}^t \neq 0} \log \left( 1 + \frac{(q_{ij}^t - \hat{q}_{ij}^t)^2}{\gamma_t^2} \right) \quad (5)$$

where  $\gamma_s$  and  $\gamma_t$  are hyper-parameters needed to be tuned externally.

Furthermore, we employ isolation forest algorithm [37] to detect the outliers present in the dataset for a given outlier ratio  $\lambda$ , where  $\lambda$  is another hyper-parameter used to decide the percentage of outliers required to be removed to evaluate the performance of our framework. In our experiment, we show the performance of TPMCF for different values of  $\lambda$ .

In the next section, we present the performance of TPMCF empirically.

## 4 EXPERIMENTS

The implementation of our framework was performed using TensorFlow v2.6.2 with Python 3.6.9. For training purposes, NVIDIA's Quadro RTX 3000/PCIe/SSE2 GPU with 1920 cores, and 6 GB memory were used. We evaluate the trained model using i9-10885H @ 2.40 GHz  $\times$  16 processor with x86\_64 CPU with 128 GB RAM. We will provide the GitHub link for our codes, if the paper gets accepted.

### 4.1 Experimental Setup

We now discuss the employed dataset followed by the performance metric, train-test split-up, and model configuration.

**Dataset description:** To validate the effectiveness of our proposed framework, we used the WSDREAM-2 [3] dataset, which comprises two QoS attributes, namely, Response Time (RT) and Throughput (TP). For both attributes, the QoS values are recorded for 64 different time-steps, each at a 15-minutes interval for globally distributed 142 users and 4500

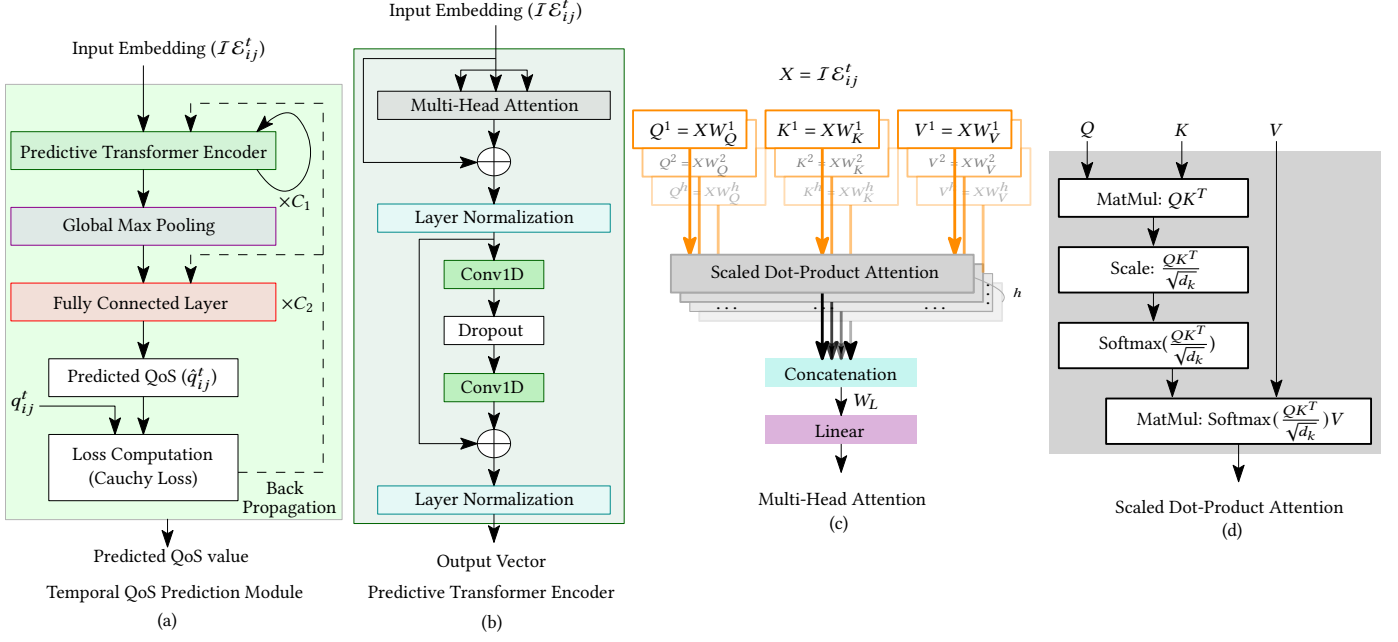


Fig. 4: Temporal QoS Prediction Module using Predictive Transformer Encoder (PTE)

TABLE 1. WSDREAM-2 dataset statistics [3]

	RT	TP		RT	TP
# User	142	142	Mean	3.177	11.345
# Service	4500	4500	Median	0.442	1.852
# Time-step	64	64	SD	6.128	54.276
Min	0.001	0.000036	Max	20.0	6726.833

SD: Standard Deviation

services. The statistical details of the dataset are shown in Table 1.

**Performance Metric:** Here, we adopted Mean Absolute Error (MAE), a widely used statistical performance metric for QoS prediction, which is defined as follows.

$$MAE = \frac{1}{|TD|} \sum_{(u_i, s_j, t_k) \in TD} |q_{ij}^k - \hat{q}_{ij}^k| \quad (6)$$

where  $TD$  is the test dataset. The smaller value for MAE indicates better accuracy.

**Train-test split-up:** In our experimentation, we used two different train-test split-ups. We divided each dataset into 10% : 90% and 20% : 80% of training-testing ratios for our experiment. Table 2 presents the details of these datasets.

TABLE 2. Dataset Description

Name	Parameter	Train : Test	Name	Parameter	Train : Test
RT-10	RT	10% : 90%	RT-20	RT	20% : 80%
TP-10	TP	10% : 90%	TP-20	TP	20% : 80%

Each experiment was performed five times. Finally, the average values were recorded and presented in this paper.

**Configuration of TPMCF:** We now present the details of various hyper-parameters of TPMCF.

**Parameter Details for Autoencoders:** We use two autoencoders (AEs) with the configuration details presented in Table 3 to generate the latent representation of the collaborative features using correlation for users and services.

**Parameters details of GCMF:** The configuration details for the GCMF are presented in Table 4.

TABLE 3. Configurations of Autoencoders

	Encoder	Decoder
No. of layers	3	3
Activation functions	$\mathcal{F}; \mathcal{T}; \ell$	$\mathcal{F}; \mathcal{T}; \ell$
Epoch	500	
Loss function	MSE	
Optimizer	Adam	
Dropout	0.4	
Patience parameter (Early stopping)	5	
Epochs	500	

Activation functions:  $\mathcal{F}$ : tanh ;  $\ell$ : linear

TABLE 4. GCMF Parameters

Parameters	Values
No. of GConv Units	2
Dimension of weight matrix $W_1^t$	$205 \times 64$
Dimension of weight matrix $W_2^t$	$64 \times 64$
Dimension of automated feature vector ( $2f'$ )	128
Optimizer	AdamW [38]
Learning rate	0.001
Loss Function	Cauchy
Activation Function	ReLU
Epochs	10000
Patience parameter (Early stopping)	300

Parameter details of PTE: The configurations of the temporal QoS prediction module with PTE are presented in Table 5.

We used  $\lambda(\text{outlier ratio}) = 0.1$  throughout our experiments unless otherwise specified. We also present a few experiments changing the values of some hyper-parameters to show their impact on prediction accuracy.

## 4.2 Experimental Analysis

We now analyze the performance of TPMCF and demonstrate the comparative study with respect to the major state-of-the-art methods (SoA).

TABLE 5. Parameters of temporal QoS prediction module

Parameters	Values	
No. of time-steps	$\mathcal{T}$	8
No. of PTE blocks	$C_1$	4
No. of heads	$h$	4
Dimension of query and key	$d_k$	256
Dimension of value	$d_v$	256
First Conv 1D	No. of filters	4
	Filter size	$3 \times 3$
	Padding	same
	Stride	1
Transformer Dropout	0.4	
Second Conv 1D	No. of filters	$\mathcal{T}$
	Filter size	$1 \times 1$
	Padding	same
	Stride	1
No. of fully connected (FC) layers	$C_2$	2
No. of nodes in each FC layer	128; 1	
Dropout	0.4	
Optimizer	AdamW [38]	
Learning rate	0.0001	
Loss Function	Cauchy	
Activation Function	ReLU	
Validation Split	0.2	
Epochs	100	
Batch Size	32	
Patience parameter (Early stopping)	10	

#### 4.2.1 Performance of TPMCF and Comparison with SoA

Here, we present the performance of TPMCF in terms of prediction time and accuracy, and the training time of the models. Table 6 presents the comparison between SoA and our framework in terms of prediction accuracy. In this table, we have categorized the SoA methods in terms of their usage of features: (a)  $QoS\_M$ : methods that used only QoS features derived from the QoS invocation log  $\mathcal{Q}$ , and (b)  $QoS\_Context\_M$ : methods employing the contextual information of users and services along with the QoS features.

**Comparison with SoA in terms of prediction accuracy:** As evident from Table 6, TPMCF outperformed all the SoA. We observed an improvement of 5.46%, 16.36%, 25.55%, and 34.02% of TPMCF over the second best SoA with QoS features as reported in Table 6 on datasets RT-10, RT-20, TP-10, and TP-20, respectively. Similarly, we reported an improvement of our framework over the second-best SoA with both the QoS and contextual features at the final row of Table 6. The final row of Table 6 shows the normalized MAE of TPMCF for all four cases of RT and TP datasets, which also shows that our framework is generalized enough.

**Comparison with SoA in terms of learning time:** Figure 5 shows the comparison between SoA and our framework

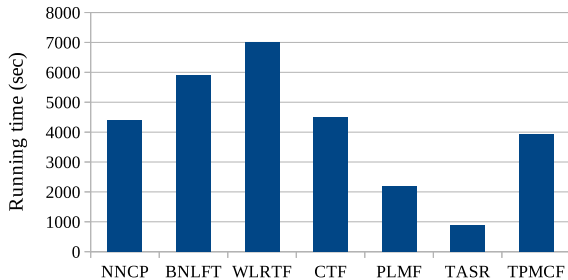


Fig. 5: Training time comparison of TPMCF with SoA

TABLE 6. Performance of TPMCF and Comparison with SoA in terms of prediction accuracy (MAE)

Category	Methods	RT-10	RT-20	TP-10	TP-20
$QoS\_M$	TASR [18]	2.8188	2.7120	4.3265	3.6419
	WSPred [19]	2.4990	2.3000	8.0131	7.6000
	OPST [26]	1.1722	1.1587	3.2762	3.1193
	BNLFT [21]	1.0828	1.0575	1.4241	1.3935
	NNCP [22]	1.0796	1.0536	2.6401	2.5797
	WLRTF [23]	1.0560	1.0437	2.9576	2.9569
	RNCF [30]	1.0100	0.9580	-	-
	CTF [20]	0.9215	0.8981	1.3567	1.1945
	CARP [39]	0.7709	0.6992	-	-
	PLMF [24]	0.6786	0.6444	-	-
	RTF [25]	0.6300	0.5350	4.0250	3.799
	DeepTQSP [29]	0.5794	0.4526	-	-
	TUIPCC [15]	0.5767	0.6970	3.7573	3.7177
GAT + GRU [40]	0.5260	0.4620	-	-	
$QoS\_Context\_M$	Mul-TSFL [27]	0.8972	0.8097	-	-
	QSPC [28]	0.8341	0.8231	3.0604	2.9624
$QoS\_M$	<b>TPMCF</b>	<b>0.4973</b>	<b>0.3864</b>	<b>1.0101</b>	<b>0.7881</b>
$QoS\_M$	<b>Improvement*</b>	<b>5.46%</b>	<b>16.36%</b>	<b>25.55%</b>	<b>34.02%</b>
$QoS\_Context\_M$	<b>Improvement*</b>	<b>40.38%</b>	<b>52.28%</b>	<b>66.99%</b>	<b>73.40%</b>
NMAE		0.1565	0.1216	0.0890	0.0695

\*Improvement over the second-best method

in terms of the training time of the models. We have the following observations from Figure 5.

(i) TPMCF had less training time as compared to four SoA methods (i.e., NNCP [22], BNLFT [21], WLRTF [23], AND CTF [20]). Out of these four methods, NNCP [22] is the fastest in terms of training time. TPMCF achieved  $1.12 \times$  speed-up and an average improvement of 62.11% over all four datasets as compared to NNCP.

(ii) CTF [20], on the other hand, is the best in terms of prediction accuracy among the four above-mentioned SoA methods. As compared to CTF, TPMCF achieved  $1.14 \times$  speed-up and an average improvement of 40.64% over all four datasets.

(iii) TPMCF was slower than PLMF [24] and TASR [18] with speed-degradation of  $0.6 \times$  and  $0.2 \times$ , respectively. However, on average, TPMCF achieved an improvement of 33.38% and 80.78% over PLMF and TASR, respectively.

**Comparison with SoA in terms of prediction time:** For TPMCF, the training is performed in offline mode. Therefore, the longer training time does not affect the actual performance of the framework. The performance of TPMCF is measured by the prediction time. The average prediction time for TPMCF is  $4.1 \times 10^{-4}$  seconds, which is reasonably well as compared to the minimum response time of the service (which is of  $10^{-3}$  seconds).

#### 4.2.2 Outlier Analysis

We now present the robustness of TPMCF in the presence of outliers. Table 7 presents the performance of TPMCF with four different loss functions for various values of the outlier ratio ( $\lambda$ ) on RT-10 dataset. It may be noted that mean-squared-error (MSE) [41] is outlier sensitive, and hence, the performance of TPMCF with MSE as the loss function was the worst. Mean-absolute-error (MAE) [42], Huber loss [43], and Cauchy loss are comparatively outlier resilient. Cauchy loss [36], however, performed the best as compared to the other loss functions, as evident from Table 7.

Table 8 presents the impact of the outliers on the prediction accuracy of TPMCF for all four datasets. As observed from Table 8, the outliers have a severe impact on the performance of TPMCF. In Figure 6, we report the performance

TABLE 7. Impact of loss function on RT-10 dataset (in terms of MAE)

Loss Function	Outlier ratio ( $\lambda$ )					
	0	0.02	0.04	0.06	0.08	0.1
MSE	0.9419	0.8443	0.7904	0.7425	0.7063	0.6796
MAE	0.8430	0.7421	0.6887	0.6417	0.6057	0.5800
Huber	0.8409	0.7384	0.6869	0.6392	0.6018	0.5742
Cauchy	0.8132	0.6985	0.6279	0.5670	0.5255	0.4973

TABLE 8. Performance (in terms of MAE) analysis over different outlier ratios ( $\lambda$ )

Datasets	Outlier ratio ( $\lambda$ )					
	0	0.02	0.04	0.06	0.08	0.1
RT-10	0.8132	0.6985	0.6279	0.5670	0.5255	0.4973
RT-20	0.6159	0.5326	0.4834	0.4399	0.4072	0.3864
TP-10	6.4200	2.7457	1.7873	1.3801	1.1490	1.0101
TP-20	5.4620	2.3853	1.5100	1.1254	0.9179	0.7881

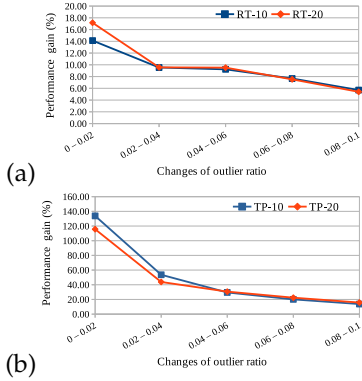


Fig. 6: Performance gain with change in outlier ratio  $\lambda$  on (a) RT and (b) TP datasets

gain with the increasing values of outlier ratio ( $\lambda$ ). As observed from Figure 6, when we removed the first 2% outliers ( $\lambda = 0.02$ ), we achieved maximum performance gain (PG) that is defined as follows:

$$PG(m_1, m_2) = \frac{m_1 - m_2}{m_2} \times 100\% \quad (7)$$

where  $m_1$  and  $m_2$  represent the MAE of TPMCF after removing outliers with the ratio  $\lambda_1$  and  $\lambda_2$ , respectively ( $\lambda_1 < \lambda_2$ ). As we removed more outliers, the performance gain gradually decreased, as evident from decreasing trends of the curves shown in Figures 6(a), (b). With the change in  $\lambda$  from 0.08 to 0.1, we achieved the least performance gain. In other words, the initial 2% outliers influenced the performance measure (i.e., MAE value) more than the rest. The rate of change of performance improvement decreased with the increase in the outlier ratio. This explains that the outlier detection algorithm is powerful enough to identify the appropriate set of outliers.

#### 4.2.3 Impact of Hyper-parameters

This section analyzes the impact a few hyper-parameters on the performance of TPMCF.

**Impact of the number of time-steps:** Figure 7(a) shows the MAE obtained by TPMCF on RT-10 dataset with the change in the number of time-steps ( $\mathcal{T}$ ) considered to construct the input embedding for the temporal QoS prediction module. We achieved the best performance for  $\mathcal{T} = 8$ . As observed

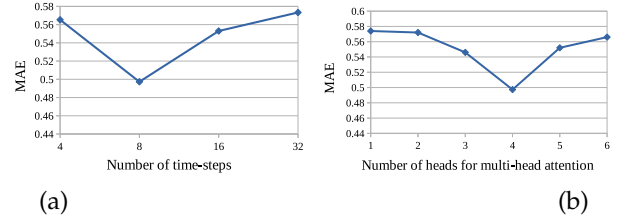


Fig. 7: Impact of (a) number of time-steps  $\mathcal{T}$ , (b) number of heads  $h$  in multi-head attention on model performance

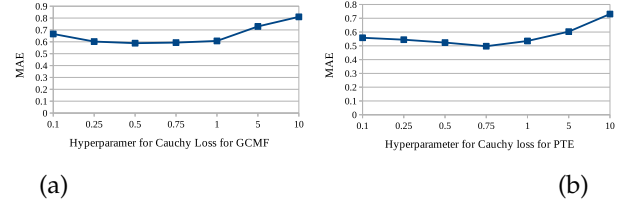


Fig. 8: Impact of (a)  $\gamma_s$  on performance of GCMF, (b)  $\gamma_t$  on performance of TPMCF

from Figure 7(a), with the increase in the value of  $\mathcal{T}$ , the MAE was decreasing till 8 time-steps, and then it started increasing for  $\mathcal{T} = 16$  and 32.

**Single vs Multi-Head Attention:** To show the impact of the number of heads ( $h$ ), we varied the value of  $h$  from 1 to 6. The results are reported in Figure 7(b) for RT-10 dataset. Initially, with the increase in the value of  $h$ , the MAE value decreased till  $h = 4$ , and it started increasing thereafter, as evident from Figure 7(b).

**Impact of  $\gamma_s$  and  $\gamma_t$ :** Figure 8(a) shows the impact of  $\gamma_s$  on the performance of GCMF on the RT-10 dataset. As observed from the figure, GCMF achieved the best prediction accuracy for  $\gamma_s = 0.5$ . Similarly, Figure 8(b) shows the impact of  $\gamma_t$  on the performance of TPMCF on the RT-10 dataset while keeping  $\gamma_s$  as constant. As observed from Figure 8(b), TPMCF achieved the best prediction accuracy for  $\gamma_t = 0.75$ .

#### 4.2.4 Ablation Study

We now present the rationale behind our model selection and the justification for having various modules of TPMCF through the ablation study.

TABLE 9. Study on Model Selection on RT-10 (in terms of MAE)

GAT+PTE	GConv+PTE	GCMF+LSTM	GCMF+GRU	TPMCF
1.1161	0.8092	0.6111	0.6171	0.4973

**Model Selection:** Table 9 presents the performance of TPMCF in terms of MAE as compared to other models that can be used to generate spatial and temporal features. We have the following observations from Table 9.

(i) We first compare GCMF with graph attention network (GAT) [44] and graph convolutional network (GConv) [45] on the RT-10 dataset. As evident from Table 9, TPMCF achieved an improvement of 55.44% and 38.54% over GAT+PTE and GConv+PTE architectures, respectively. This experiment shows the effectiveness of GCMF in TPMCF.

(ii) We further implemented the temporal QoS prediction block using LSTM [46] and GRU [47]. TPMCF achieved an improvement of 18.62% and 19.41% over GCMF+LSTM and

GCMF+GRU architectures, respectively. This experiment explains the importance of the PTE as part of the temporal QoS prediction block.

TABLE 10. Module ablation study (in terms of MAE)

Datasets	Features		
	Spatial	Temporal	Spatial + Temporal
	GCMF	PTE	TPMCF
RT-10	0.5884	0.5842	0.4973
RT-20	0.4762	0.4796	0.3864
TP-10	1.1616	1.1879	1.0101
TP-20	0.8877	0.8506	0.7881

**Module Ablation:** Table 10 presents the ablation study for various modules in TPMCF. We have the following observations from Table 10.

(i) TPMCF achieved on average 14.65% improvement over the stand-alone GCMF, which justifies the requirement of temporal QoS prediction block.

(ii) TPMCF achieved on average 14.16% improvement over the stand-alone transformer encoder with temporal features. This implies the necessity of capturing the spatial features along with the temporal dependencies.

**Feature Ablation:** Table 11 presents the feature ablation study for TPMCF. As observed from Table 11, TPMCF with the combined features outperformed the same model with individual feature categories, as discussed in Section 3.1.1. On the one hand, this experiment shows the significance of using the collaborative features derived from domain knowledge apart from the other auto-extracted features used for QoS prediction. On the other hand, it justifies using the different sets of features extracted to employ in TPMCF.

TABLE 11. Feature ablation study (in terms of MAE)

Datasets	Statistical Features	QoS Features	Collaborative Features using Correlations	Combined Features
RT-10	0.5939	0.5821	0.5771	0.4973
RT-20	0.4517	0.4093	0.4104	0.3864
TP-10	1.4249	1.1350	1.0891	1.0101
TP-20	1.1112	0.8281	0.8590	0.7881

In summary, TPMCF achieved higher prediction accuracy than the SoA methods while ensuring reasonably good prediction time.

## 5 RELATED WORKS

In this section, we present a brief literature survey on QoS prediction. We broadly classify the QoS prediction into two categories: static and dynamic. We illustrate each of these categories below.

### 5.1 Static QoS Prediction

In static QoS prediction, we assume the QoS parameter of service varies across users [48], [49]. Collaborative filtering (CF) is one of the primary techniques to solve static QoS prediction problems. The SoA methods explore various CF-based approaches (e.g., similarity-based [7], [8], [9], matrix factorization-based [10], [11], [50], [51], factorization machine-based [12], [13], [52], deep architecture-based [5]) to address various issues (e.g., scalability [53], cold-start [4], [50], data sparsity [4], [14], trustworthiness of users/services [54], [55]) in the static QoS prediction problem to achieve high prediction accuracy, faster responsiveness, or high

scalability [2], [6]. However, the QoS parameter for a user-service pair hardly remains constant; it fluctuates over time because of several factors, such as service status (e.g., workload, number of users accessing the service simultaneously), network congestion, etc. [19], [20]. Therefore, these static methods fail to predict the QoS value in a dynamic QoS environment.

### 5.2 Dynamic/ Temporal QoS Prediction

Dynamic QoS prediction, also referred to as temporal QoS prediction, considers the temporal dependency among QoS data. We now present various SoA strategies for tackling temporal QoS problems.

#### 5.2.1 Temporal Smoothing (TS)-based QoS Prediction

TUIPCC [15] and TF-KMP [16] leveraged similarity-based CF to fill up the missing values in temporal QoS invocation log and then computed weighted average of QoS data across previous time-steps. Meanwhile, another TS-based method TMF [17] employed the user-service latent factors in data-imputation method instead of using similarity-based CF. However, TS-based methods are not able to capture the complex features over temporal QoS invocation sequences accurately, and thereby hardly achieve desirable prediction accuracy.

#### 5.2.2 ARIMA-based QoS Prediction

TASR [18] proposed a time-aware and sparsity-tolerant approach to capture the temporal features using a traditional ARIMA-based time-series forecasting model. However, ARIMA-based models are computationally expensive, assume time series data as stationary, and suffer from low accuracy in long-term forecasts involving a large number of time-steps.

#### 5.2.3 Tensor Factorization (TF)-based QoS Prediction

WSPred [19] first proposed a tensor factorization method leveraging the latent features among the users, services and time-steps. The methods in [19], [21], [22] employed a low-rank tensor factorization to obtain user, services, and time latent features for predicting QoS value. These methods used squared error loss as the objective function with the regularization term, resulting in low prediction accuracy due to the usage of outlier sensitive loss function. To address the outlier issue, CTF [20] engaged non-negative TF to learn the latent vectors using a multiplicative updating algorithm with Cauchy loss [36], which is comparatively robust to the outliers. In general, TF-based methods experience accuracy degradation due to their inability to capture an effective representation of implicit features.

#### 5.2.4 Deep Architecture (DA)-based QoS Prediction

Recurrent neural network-based architectures are able to extract the temporal features in sequence-to-sequence fashion. The deep architectures for sequence modeling, such as LSTM [46] or GRU [47] are primarily used for the time-aware QoS prediction [24], [25], [26], [27], [28], [29], [30]. Mul-TSFL [27] leveraged contextual features (e.g., geolocation, autonomous system number, and country information of users/services) to fill up missing values and employed

TABLE 12. Literature survey for temporal QoS prediction

Method	Technique	Explicit Features		Auto-extracted features	
		QoS	Contextual	Spatial	Temporal
TMF [17]	Temporal smoothing	MF	-	-	-
TF-KMP [16]		Similarity	-	-	-
TUIPCC [15]			-	-	-
WLRTF [23]	Tensor factorization	TF/NTF	-	-	-
WSPred [19]			-	-	-
BNLFT [21]			-	-	-
NNCP [22]			-	-	-
CTF [20]			-	-	-
TASR [18]	ARIMA	Similarity	-	-	Yes
OPST [26]	LSTM	MF	-	-	Yes
PLMF [24]			Location, IP	-	Yes
Mu-TSFL [27]		Similarity	Location, AS	-	Yes
QSPC [28]		-	ID, AS, URL	-	Yes
RNCF [30]		GRU	Similarity	-	-
DeepTSQP [29]	-			-	Yes
RTF [25]	TF			-	-
GAT+GRU [40]	GAT + GRU	-	-	Yes	Yes
TPMCF	GCMF + PTE	Similarity + MF + Statistical features	-	Yes	Yes

AS: Autonomous System, NTF: Non-negative Tensor Factorization, MF: Matrix Factorization, TF: Tensor Factorization

a multivariate LSTM model to capture temporal features. DeepTSQP [29] used binary invocation and similarity features with GRU to capture the temporal features for QoS prediction. PLMF [24] proposed an online temporal QoS prediction framework utilizing the LSTM model to predict the QoS of multiple services for a user at a time, which further tackled the cold-start problem. In general, LSTM and GRU-based models outperform the TS, ARIMA, and TF-based methods. However, the prediction accuracy of DA-based models are still not up to the mark due to the usage of hand-crafted features and the inability to capture complex relations among data. Moreover, they suffer from high convergence time, low learning efficiency, and high memory requirement.

We now discuss various features used in the literature for temporal QoS prediction and their impact and limitations.

### 5.3 Various Feature Representation for QoS Prediction

The features that have been used in the literature are broadly classified into two categories explicit features extracted using domain knowledge and auto-extracted features. The explicit features can be either QoS features or contextual features. Similarly, the auto-extracted features can be spatial or temporal. We now discuss each of the categories in detail.

#### 5.3.1 QoS Features

The QoS features are usually derived from the QoS invocation log. In general, the QoS feature includes the QoS profile of a given target user-service pair, which depicts the behavior of the user/service in terms of the QoS parameter. A few examples of QoS features are as follows: statistical features (e.g., mean, median, min, max, the variance of the QoS invocation profile of user/service) [45], the similarity between users/services [15], [16], and features generated by matrix factorization [21], [26]. The majority of the work in the literature has used various QoS features for temporal QoS prediction [24], [27], [30]. However, the collaborative information of other users/services is mostly missing in the QoS feature of a target user/service. Moreover, the QoS features generally do not contain any temporal information.

Therefore, achieving high accuracy by only using QoS features is difficult.

#### 5.3.2 Contextual Features

A few methods in the literature have used the contextual features derived from the contextual information of users/services (e.g., latitude, longitude, country, autonomous system, IP of users/services) [27], [28]. Although the contextual information may reveal some additional useful information about users and services, the availability of the contextual information for all the users and services is challenging.

#### 5.3.3 Spatial Features

Spatial features capture information regarding neighborhood relationships. In some papers, the features extracted from the location of users/services are referred to as spatial features [27], [28]. However, this paper has categorized the location information as contextual data. A few papers auto-extracted spatial features to improve the prediction accuracy by exploring the neighborhood relationships using graph convolution. For example, TAN [49] leveraged the network topology among the users and services by using IPs and ASs, used graph convolution to capture the cross-correlation among them and employed the BiLSTM for QoS prediction. However, they had to remove a significant number of users/services from the experiment due to the absence of contextual information (e.g., IPs, ASs). HSA Net [48] proposed a privacy-preserving QoS prediction method to learn the spatial features using a convolution neural network with the known users/services information and hidden state features obtained using Latent Dirichlet Allocation (LDA). TRQP [45] employed a graph convolution network and extracted the spatial features for static QoS prediction. However, none of these works captured any temporal dependencies. These works mainly focused on solving the static QoS prediction problem. Hence, these methods are not recommended to solve the dynamic prediction problem.

#### 5.3.4 Temporal Features

A few recent methods auto-extracted the temporal features for dynamic QoS prediction. For example, DeepTSQP [29]

leveraged GRU [47] to learn the user-service invocation features with similarity features. RTF [25] used GRU with tensor factorization features. RNCF [30] employed neural collaborative filtering with GRU. PLMF [24] used matrix decomposition features for online QoS prediction. However, none of these methods thoroughly explore the collaborative relationship between users/services and, therefore, left the scope to improve prediction accuracy.

In addition to the temporal features, a few methods have used contextual information (e.g., location, IP, ID) of the target user/service for prediction [27], [28]. As discussed earlier, contextual information is not always available to model the QoS prediction problem.

### 5.3.5 Spatio-temporal Features

A very recent paper [40] has considered spatio-temporal features for QoS prediction, where a graph attention network was used to capture spatial features, and GRU was used to capture temporal dependencies. However, in addition to the spatio-temporal features, the explicit features using domain knowledge may improve prediction accuracy, which was unexplored in [40].

Table 12 summarizes a study on various feature representation for temporal QoS prediction.

## 5.4 Positioning Our Framework TPMCF

In contrast to the past SoA methods, TPMCF thoroughly exploits the collaborative features among users/services through explicit features derived from domain knowledge and auto-extracted spatio-temporal features. These features together can capture higher-order, complex relationships among QoS data, enabling our framework to attain high prediction accuracy. TPMCF employs a predictive transformer encoder (PTE) that provides attention to the user-service interactions over time, which is missing in classical LSTM/GRU-based sequential architectures. Using GCMF to extract spatial features adds more value to our work and improves prediction accuracy. Experimentally, we have shown that GCMF performed better than the contemporary graph convolution [45] or graph attention network [40], [44].

Additionally, by using Cauchy loss as the objective function, we make TPMCF outlier resilient. The offline training of GCMF and temporal QoS prediction module does not influence prediction time, which ensures faster responsiveness during prediction. Furthermore, the latent feature representation obtained from autoencoders to train the GCMF module helps attain high scalability.

## 6 CONCLUSION

This paper presents an efficient solution for temporal QoS prediction for service recommendation. Specifically, our framework (TPMCF) leverages multi-source collaborative features comprising explicit features derived using domain knowledge and auto-extracted spatio-temporal features. TPMCF includes a collaborative spatial feature-extraction module (CSFE) and a temporal QoS prediction module (TQP). CSFE is responsible for spatial feature extraction using graph convolutional matrix factorization (GCMF). On the other hand, TQP is accountable for temporal feature

extraction using a predictive transformer encoder (PTE), followed by QoS prediction using a fully connected neural network. To our best knowledge, TPMCF is the very first QoS prediction method that exploits the transformer encoder network for capturing the triadic relationships among the users, services and time-steps for service recommendation.

Additionally, TPMCF is competent in addressing a few fundamental challenges in temporal QoS prediction. For example, to deal with the outliers present in the datasets, TPMCF employs Cauchy loss to train the GCMF and PTE. TPMCF is sparsity-tolerant without using any additional data imputation method due to GCMF. The offline training of GCMF and PTE ensures the high responsiveness of TPMCF. This makes TPMCF a better fit for real-time applications. Moreover, the feature dimensionality reduction with the help of autoencoders makes TPMCF highly scalable.

Our extensive experiments on WSDREAM-2 datasets show that we achieved higher prediction accuracy than the major state-of-the-art methods, while having reasonably faster training time as compared to other contemporary methods, and negligible prediction time with respect to the response time of the services.

Although TPMCF achieved high prediction accuracy, there is still scope for improvement. There are a few challenges, which are unaddressed in our paper, for example, the analysis of the trustworthiness of users and services to exploit collaborative relationships. As our future endeavor, we aim to propose a trust-aware temporal QoS prediction framework.

## REFERENCES

- [1] T. Erl, *Service-oriented architecture: a field guide to integrating XML and web services*. Prentice Hall PTR, 2004.
- [2] Z. Zheng, X. Li, M. Tang, F. Xie, and M. R. Lyu, "Web service qos prediction via collaborative filtering: A survey," *IEEE Transactions on Services Computing*, vol. 15, no. 4, pp. 2455–2472, 2022.
- [3] Z. Zheng, Y. Zhang, and M. R. Lyu, "Investigating qos of real-world web services," *IEEE Transactions on Services Computing*, vol. 7, no. 1, pp. 32–39, 2014.
- [4] S. Chattopadhyay, R. Chanda, S. Kumar, and C. Adak, "Offdq: An offline deep learning framework for qos prediction," in *Proceedings of the ACM Web Conference 2022*, ser. WWW '22. New York, NY, USA: Association for Computing Machinery, 2022, p. 1987–1996. [Online]. Available: <https://doi.org/10.1145/3485447.3512107>
- [5] Y. Yin, Z. Cao, Y. Xu, H. Gao, R. Li, and Z. Mai, "Qos prediction for service recommendation with features learning in mobile edge computing environment," *IEEE Transactions on Cognitive Communications and Networking*, vol. 6, no. 4, pp. 1136–1145, 2020.
- [6] S. H. Ghafouri, S. M. Hashemi, and P. C. K. Hung, "A survey on web service qos prediction methods," *IEEE Transactions on Services Computing*, vol. 15, no. 4, pp. 2439–2454, 2022.
- [7] J. S. Breese, D. Heckerman, and C. Kadie, "Empirical analysis of predictive algorithms for collaborative filtering," in *Proc. of the 14th Conference on Uncertainty in Artificial Intelligence*, ser. UAI'98, 1998, p. 43–52.
- [8] B. Sarwar, G. Karypis, J. Konstan, and J. Riedl, "Item-based collaborative filtering recommendation algorithms," in *Proceedings of the 10th International Conference on World Wide Web*, ser. WWW '01. New York, NY, USA: Association for Computing Machinery, 2001, p. 285–295. [Online]. Available: <https://doi.org/10.1145/371920.372071>
- [9] Z. Zheng, H. Ma, M. R. Lyu, and I. King, "Qos-aware web service recommendation by collaborative filtering," *IEEE Transactions on Services Computing*, vol. 4, no. 2, pp. 140–152, 2011.
- [10] D. D. Lee and H. S. Seung, "Learning the parts of objects by non-negative matrix factorization," *Nature*, vol. 401, pp. 788–791, 1999.

- [11] Z. Zheng, H. Ma, M. R. Lyu, and I. King, "Collaborative web service qos prediction via neighborhood integrated matrix factorization," *IEEE Transactions on Services Computing*, vol. 6, no. 3, pp. 289–299, 2013.
- [12] L. Shen, M. Pan, L. Liu, D. You, F. Li, and Z. Chen, "Contexts enhance accuracy: On modeling context aware deep factorization machine for web api qos prediction," *IEEE Access*, vol. 8, pp. 165 551–165 569, 2020.
- [13] Y. Wu, F. Xie, L. Chen, C. Chen, and Z. Zheng, "An embedding based factorization machine approach for web service qos prediction," in *Service-Oriented Computing*, M. Maximilien, A. Vallecillo, J. Wang, and M. Oriol, Eds. Cham: Springer International Publishing, 2017, pp. 272–286.
- [14] R. R. Chowdhury, S. Chattopadhyay, and C. Adak, "Cahphf: Context-aware hierarchical qos prediction with hybrid filtering," *IEEE Transactions on Services Computing*, vol. 15, no. 4, pp. 2232–2247, 2022.
- [15] E. Tong, W. Niu, and J. Liu, "A missing qos prediction approach via time-aware collaborative filtering," *IEEE Transactions on Services Computing*, pp. 1–1, 2021.
- [16] C. Wu, W. Qiu, X. Wang, Z. Zheng, and X. Yang, "Time-aware and sparsity-tolerant qos prediction based on collaborative filtering," in *2016 IEEE International Conference on Web Services (ICWS)*, 2016, pp. 637–640.
- [17] S. Li, J. Wen, F. Luo, and G. Ranzi, "Time-aware qos prediction for cloud service recommendation based on matrix factorization," *IEEE Access*, vol. 6, pp. 77 716–77 724, 2018.
- [18] S. Ding, Y. Li, D. Wu, Y. Zhang, and S. Yang, "Time-aware cloud service recommendation using similarity-enhanced collaborative filtering and arima model," *Decis. Support Syst.*, vol. 107, no. C, p. 103–115, mar 2018. [Online]. Available: <https://doi.org/10.1016/j.dss.2017.12.012>
- [19] Y. Zhang, Z. Zheng, and M. R. Lyu, "Wspread: A time-aware personalized qos prediction framework for web services," in *2011 IEEE 22nd International Symposium on Software Reliability Engineering*, 2011, pp. 210–219.
- [20] F. Ye, Z. Lin, C. Chen, Z. Zheng, and H. Huang, "Outlier-resilient web service qos prediction," in *Proceedings of the Web Conference 2021*, ser. WWW '21. New York, NY, USA: Association for Computing Machinery, 2021, p. 3099–3110. [Online]. Available: <https://doi.org/10.1145/3442381.3449938>
- [21] X. Luo, H. Wu, H. Yuan, and M. Zhou, "Temporal pattern-aware qos prediction via biased non-negative latent factorization of tensors," *IEEE Transactions on Cybernetics*, vol. 50, no. 5, pp. 1798–1809, 2020.
- [22] W. Zhang, H. Sun, X. Liu, and X. Guo, "Temporal qos-aware web service recommendation via non-negative tensor factorization," in *Proceedings of the 23rd International Conference on World Wide Web*, ser. WWW '14. New York, NY, USA: Association for Computing Machinery, 2014, p. 585–596. [Online]. Available: <https://doi.org/10.1145/2566486.2568001>
- [23] X. Chen, Z. Han, Y. Wang, Q. Zhao, D. Meng, and Y. Tang, "Robust tensor factorization with unknown noise," in *2016 IEEE Conference on Computer Vision and Pattern Recognition (CVPR)*, 2016, pp. 5213–5221.
- [24] R. Xiong, J. Wang, Z. Li, B. Li, and P. C. K. Hung, "Personalized lstm based matrix factorization for online qos prediction," in *2018 IEEE International Conference on Web Services (ICWS)*, 2018, pp. 34–41.
- [25] Y. Zhang, C. Yin, Z. Lu, D. Yan, M. Qiu, and Q. Tang, "Recurrent tensor factorization for time-aware service recommendation," *Appl. Soft Comput.*, vol. 85, no. C, dec 2019. [Online]. Available: <https://doi.org/10.1016/j.asoc.2019.105762>
- [26] G. White, A. Palade, C. Cabrera, and S. Clarke, "Autoencoders for qos prediction at the edge," in *2019 IEEE International Conference on Pervasive Computing and Communications (PerCom)*, 2019, pp. 1–9.
- [27] M. Wang, B. Liu, J. Li, Y. Li, H. Chen, Z. Zhou, and W. Zhang, "A location-based approach for web service qos prediction via multivariate time series forecast," in *2020 IEEE 11th International Conference on Software Engineering and Service Science (ICSESS)*, 2020, pp. 36–39.
- [28] B. Li, C. Ye, X. Yu, H. Zhou, and C. Huang, "Qos prediction based on temporal information and request context," *Serv. Oriented Comput. Appl.*, vol. 15, no. 3, p. 231–244, sep 2021. [Online]. Available: <https://doi.org/10.1007/s11761-021-00322-4>
- [29] G. Zou, T. Li, M. Jiang, S. Hu, C. Cao, B. Zhang, Y. Gan, and Y. Chen, "Deeptsq: Temporal-aware service qos prediction via deep neural network and feature integration," *Know.-Based Syst.*, vol. 241, no. C, apr 2022. [Online]. Available: <https://doi.org/10.1016/j.knosys.2021.108062>
- [30] T. Liang, M. Chen, Y. Yin, L. Zhou, and H. Ying, "Recurrent neural network based collaborative filtering for qos prediction in iov," *IEEE Transactions on Intelligent Transportation Systems*, vol. 23, no. 3, pp. 2400–2410, 2022.
- [31] T. N. Kipf and M. Welling, "Semi-supervised classification with graph convolutional networks," in *5th International Conference on Learning Representations, ICLR 2017, Toulon, France, April 24–26, 2017, Conference Track Proceedings*. OpenReview.net, 2017.
- [32] A. Vaswani, N. Shazeer, N. Parmar, J. Uszkoreit, L. Jones, A. N. Gomez, L. Kaiser, and I. Polosukhin, "Attention is all you need," in *Proceedings of the 31st International Conference on Neural Information Processing Systems*, ser. NIPS'17. Red Hook, NY, USA: Curran Associates Inc., 2017, p. 6000–6010.
- [33] H. V. Nguyen and L. Bai, "Cosine similarity metric learning for face verification," in *Asian conference on computer vision*. Springer, 2010, pp. 709–720.
- [34] P. Vincent, H. Larochelle, I. Lajoie, Y. Bengio, and P.-A. Manzagol, "Stacked denoising autoencoders: Learning useful representations in a deep network with a local denoising criterion," *J. Mach. Learn. Res.*, vol. 11, p. 3371–3408, dec 2010.
- [35] A. Zhang, Z. C. Lipton, M. Li, and A. J. Smola, "Dive into deep learning," *arXiv preprint arXiv:2106.11342*, 2021.
- [36] X. Li, Q. Lu, Y. Dong, and D. Tao, "Robust subspace clustering by cauchy loss function," *IEEE Transactions on Neural Networks and Learning Systems*, vol. 30, no. 7, pp. 2067–2078, 2019.
- [37] F. T. Liu, K. M. Ting, and Z.-H. Zhou, "Isolation-based anomaly detection," *ACM Trans. Knowl. Discov. Data*, vol. 6, no. 1, mar 2012. [Online]. Available: <https://doi.org/10.1145/2133360.2133363>
- [38] I. Loshchilov and F. Hutter, "Decoupled weight decay regularization," in *7th International Conference on Learning Representations, ICLR 2019, New Orleans, LA, USA, May 6–9, 2019*. OpenReview.net, 2019.
- [39] J. Zhu, P. He, Q. Xie, Z. Zheng, and M. R. Lyu, "CARP: context-aware reliability prediction of black-box web services," in *2017 IEEE International Conference on Web Services, ICWS 2017, Honolulu, HI, USA, June 25–30, 2017*, I. Altintas and S. Chen, Eds. IEEE, 2017, pp. 17–24.
- [40] S. Hu et al., "Temporal-aware qos prediction via dynamic graph neural collaborative learning," in *Service-Oriented Computing - 20th International Conference, ICSOC 2022, Seville, Spain, November 29 - December 2, 2022, Proceedings*, ser. Lecture Notes in Computer Science, vol. 13740. Springer, 2022, pp. 125–133.
- [41] Z. Wang and A. C. Bovik, "Mean squared error: Love it or leave it? a new look at signal fidelity measures," *IEEE signal processing magazine*, vol. 26, no. 1, pp. 98–117, 2009.
- [42] C. J. Willmott and K. Matsuura, "Advantages of the mean absolute error (mae) over the root mean square error (rmse) in assessing average model performance," *Climate research*, vol. 30, no. 1, pp. 79–82, 2005.
- [43] P. J. Huber, *Robust Estimation of a Location Parameter*. New York, NY: Springer New York, 1992, pp. 492–518. [Online]. Available: [https://doi.org/10.1007/978-1-4612-4380-9\\_35](https://doi.org/10.1007/978-1-4612-4380-9_35)
- [44] P. Velickovic, G. Cucurull, A. Casanova, A. Romero, P. Liò, and Y. Bengio, "Graph attention networks," in *6th International Conference on Learning Representations, ICLR 2018, Vancouver, BC, Canada, April 30 - May 3, 2018, Conference Track Proceedings*. OpenReview.net, 2018.
- [45] S. Kumar and S. Chattopadhyay, "TRQP: trust-aware real-time qos prediction framework using graph-based learning," in *Service-Oriented Computing - 20th International Conference, ICSOC 2022, Seville, Spain, November 29 - December 2, 2022, Proceedings*, ser. Lecture Notes in Computer Science, vol. 13740. Springer, 2022, pp. 143–152.
- [46] S. Hochreiter and J. Schmidhuber, "Long short-term memory," *Neural Comput.*, vol. 9, no. 8, p. 1735–1780, nov 1997. [Online]. Available: <https://doi.org/10.1162/neco.1997.9.8.1735>
- [47] J. Chung, Ç. Gülçehre, K. Cho, and Y. Bengio, "Empirical evaluation of gated recurrent neural networks on sequence modeling," *CoRR*, vol. abs/1412.3555, 2014. [Online]. Available: <http://arxiv.org/abs/1412.3555>
- [48] Z. Wang, X. Zhang, M. Yan, L. Xu, and D. Yang, "Hsa-net: Hidden-state-aware networks for high-precision qos prediction," *IEEE Trans. Parallel Distributed Syst.*, vol. 33, no. 6, pp. 1421–1435, 2022.

- [49] J. Li, H. Wu, J. Chen, Q. He, and C. Hsu, "Topology-aware neural model for highly accurate qos prediction," *IEEE Trans. Parallel Distributed Syst.*, vol. 33, no. 7, pp. 1538–1552, 2022.
- [50] W. Lo, J. Yin, S. Deng, Y. Li, and Z. Wu, "An extended matrix factorization approach for qos prediction in service selection," in *2012 IEEE Ninth International Conference on Services Computing*, 2012, pp. 162–169.
- [51] R. Salakhutdinov and A. Mnih, "Probabilistic matrix factorization," in *Proceedings of the 20th International Conference on Neural Information Processing Systems*, ser. NIPS'07. Red Hook, NY, USA: Curran Associates Inc., 2007, p. 1257–1264.
- [52] M. Li, Q. Lu, and M. Zhang, "A two-tier service filtering model for web service qos prediction," *IEEE Access*, vol. 8, pp. 221 278–221 287, 2020.
- [53] C. Yu and L. Huang, "Clucf: A clustering cf algorithm to address data sparsity problem," *Serv. Oriented Comput. Appl.*, vol. 11, no. 1, p. 33–45, mar 2017. [Online]. Available: <https://doi.org/10.1007/s11761-016-0191-8>
- [54] C. Wu, W. Qiu, Z. Zheng, X. Wang, and X. Yang, "Qos prediction of web services based on two-phase k-means clustering," in *2015 IEEE International Conference on Web Services*, 2015, pp. 161–168.
- [55] K. Su, B. Xiao, B. Liu, H. Zhang, and Z. Zhang, "Tap: A personalized trust-aware qos prediction approach for web service recommendation," *Knowledge-Based Systems*, vol. 115, pp. 55–65, 2017. [Online]. Available: <https://www.sciencedirect.com/science/article/pii/S0950705116303331>



**Suraj Kumaer** received his B.Tech and M.Tech in Computer Science and Engineering (CSE) from Aligarh Muslim University, Aligarh, India, in 2017 and 2019 respectively. Currently, he is pursuing his PhD in CSE from the Indian Institute of Information Technology Guwahati (IIIT Guwahati), India. His research interests include Web Services Computing, Machine Learning, Deep Learning, and Graph Representation Learning.



**Soumi Chattopadhyay** (Member, IEEE) received her PhD from Indian Statistical Institute, Kolkata in 2019. Currently, she is an Assistant Professor at the Indian Institute of Information Technology Guwahati (IIIT Guwahati), India. Her research interests include Distributed and Services Computing, Artificial Intelligence, Formal Languages, Logic and Reasoning.



**Chandranath Adak** (Senior Member, IEEE) received his PhD in Analytics from the University of Technology Sydney, Australia in 2019. Currently, he is an Assistant Professor at the Indian Institute of Technology Patna (IIT Patna), India. His research interests include Computer Vision, Pattern Recognition, Document Image Analysis, and Machine Learning.